

# Near-Infrared-Emitting Five-Monolayer Thick Copper-Doped CdSe Nanoplatelets

Ashma Sharma, Manoj Sharma, Kivanc Gungor, Murat Olutas, Didem Dede, and Hilmi Volkan Demir\*

Doped nanocrystals are instrumental to the high-performance luminescent solar concentrators (LSCs) and the color conversion devices. Recently, copper (Cu)-doped three and four monolayer (ML) thick CdSe nanoplatelets (NPLs) have been shown superior to the existing Cu-doped quantum dots (QDs) for their use in LSCs. However, additional improvement in the LSC performance can be achieved by further redshifting the emission into the near-infrared (NIR) region of electromagnetic spectrum and increasing the absorbed portion of the solar irradiation. Cu-doping into higher thicknesses of these atomically flat NPLs (e.g.,  $\geq 5$  ML) can achieve these overarching goals. However, addition of the dopant ions during the nucleation stage disturbs this high-temperature growth process and leads to multiple populations of NPLs and QDs. Here, by carefully controlling the precursor chemistry the successful doping of Cu in five ML thick NPLs by high-temperature nucleation doping method is demonstrated. The optimized synthesis method shows nearly pure population of doped five ML thick NPLs, which possess  $\approx 150$  nm Stokes-shifted NIR emission with high quantum yield of  $65 \pm 2\%$ . Structural, elemental, and optical studies are conducted to confirm the successful doping and understand the detailed photophysics. Finally, these materials are tested experimentally and theoretically for their performance as promising LSC materials.

## 1. Introduction

Copper doping in the semiconductor nanocrystals (NCs) has been fascinating much attention nowadays, which offers high performance in a variety of optoelectronic applications.<sup>[1–4]</sup> In the last two decades lots of work has been done on doping of Cu in NCs of different materials, e.g., ZnSe, ZnS, CuInS, and CdSe.<sup>[2,4–11]</sup> Doping of Cu(I) typically creates a mid-band-gap state in the band gap of the host semiconductor NCs, which captures the photoexcited holes and thus allows a radiative recombination of photogenerated electrons in the conduction band.<sup>[2,12,13]</sup> These doped NCs possess a broadband and tunable visible to near-infrared (NIR) dopant induced emission, nearly zero self-absorption, high photoluminescence (PL) quantum yield (QY), and p-type conductivity, which make these NCs one of the promising candidates for their possible use in luminescent solar concentrators (LSCs), light-emitting diodes, color conversion devices, lasers, and optical fibers.<sup>[1–3,14–16]</sup>

Recently Gamelin et al. studied different NC phosphors for their possible application as LSC emitters.<sup>[1]</sup> This study demonstrates Cu-doped CdSe quantum dots (QDs) as the most suitable material for LSCs as compared to widely studied Mn-doped ZnCdS/ZnS QDs, CdSe/CdS dots in rods, and CdSe/CdS giant QDs. Cu-doped CdSe QDs possess moderate PL QYs (20%–30%), large Stokes shift, NIR emission, and higher absorption overlap with the solar spectrum, which altogether boosts their performance in LSCs. Very recently, Cu-doped three to four monolayer (ML) CdSe nanoplatelets (NPLs) were added into the family of colloidal quantum wells that possess extraordinarily high PL QYs (80%–90%), large Stokes-shifted NIR emission, high absorption cross-sections, and step-like optical absorption profiles.<sup>[15]</sup> As compared to colloidal QDs, CdSe NPLs by exploiting the atomically precise and identical thicknesses effectively eliminate the inhomogeneous broadening of the absorption and emission spectra.<sup>[17,18]</sup> This also leads to ideal step-like absorption profiles. These extraordinary properties allow the doped NPLs to find use for solar light harvesting applications.<sup>[15]</sup> However, for further improvement in the performance of these doped NPLs as LSC materials, their

A. Sharma, Dr. M. Sharma, Dr. K. Gungor, Dr. M. Olutas, D. Dede, Prof. H. V. Demir  
Department of Electrical and Electronics Engineering  
Department of Physics  
UNAM-Institute of Materials Science and Nanotechnology  
Bilkent University  
Ankara 06800, Turkey  
E-mail: volkan@bilkent.edu.tr, hvdemir@ntu.edu.sg

A. Sharma, Dr. M. Sharma, Prof. H. V. Demir  
Luminous! Center of Excellence for Semiconductor  
Lighting and Displays  
School of Electrical and Electronic Engineering  
School of Physical and Mathematical Sciences  
School of Materials Science and Engineering  
Nanyang Technological University  
Singapore 639798, Singapore

Dr. M. Olutas  
Department of Physics  
Abant İzzet Baysal University  
Bolu 14030, Turkey

 The ORCID identification number(s) for the author(s) of this article can be found under <https://doi.org/10.1002/adom.201900831>.

DOI: 10.1002/adom.201900831

emission spectrum has to be further shifted into NIR region and their optical absorption overlap with the solar irradiation has to be increased.<sup>[1,19]</sup> In order to realize this goal, doping in thick NPLs ( $\geq 5$  ML) is a requisite. The typical temperature for the synthesis of Cu-doped QDs and three to four ML NPLs using cluster seeded and high-temperature nucleation doping methods was around 180–240 °C.<sup>[12,15,20]</sup> However, the synthesis of undoped five ML CdSe NPLs as reported in the literature requires a higher temperature ( $\approx 250$  °C).<sup>[21]</sup> Thus addition of the dopant ions at such a high temperature may disturb the nucleation and growth process. Therefore, for the successful doping of Cu dopant ions in  $\geq 5$  ML NPLs, a careful control of reaction kinetics and reactivity of the dopant precursors is needed. Furthermore, new low-temperature synthesis methods for doping in CdSe NPLs could be explored. Earlier, we reported Cu(I) doping in three to five ML CdSe NPLs by using a partial cation exchange (CE) method and used them to study the dopant induced orbital hybridization of the host energy levels.<sup>[13]</sup> Recently, this partial CE has also been extended to Ag doping in CdSe NPLs.<sup>[22,23]</sup> However, the typical PL QYs for Cu-doped NPLs synthesized using a partial CE method are low as compared to the high-temperature methods.<sup>[1,13,15,24]</sup> To the best of our knowledge there is no report of doping in five ML thick CdSe NPLs by a high-temperature nucleation doping method.

Here, we show for the first time the successful synthesis of five ML Cu-doped CdSe NPLs via a nucleation doping method. By carefully controlling the reactivity of the dopant ions during the nucleation, we achieved a nearly pure population of five ML Cu-doped CdSe NPLs possessing an efficient and NIR emission. Different dopant precursors with variable TOP/Cu ratios were tried to achieve the successful synthesis. Moreover, the dopant emission contribution and tuning the emission spectrum in further NIR region is achieved with a new two-step doping procedure. Furthermore, detailed optical studies by steady-state and time-resolved spectroscopies and structural and elemental studies by inductively coupled plasma mass spectroscopy (ICP-MS), high-angle annular dark-field scanning transmission electron microscopy (STEM), and X-ray photoelectron spectroscopy (XPS) prove the successful Cu doping into these thicker NPLs by the nucleation doping method. Thereafter, these Cu-doped NPLs possessing high absorption cross-section and high PL QYs were tested for reabsorption studies using an earlier reported 1D liquid waveguide setup.<sup>[1,15,25,26]</sup> Finally, the performance of these five ML Cu-doped NPLs has been compared with previously studied thinner doped NPLs, and future perspective has been presented for the further improvements.

## 2. Results and Discussions

Atomically flat undoped CdSe NPLs having five ML vertical thicknesses were synthesized by using a pre-existing synthesis recipe.<sup>[18,27]</sup> However, for the doping of Cu in five ML thick CdSe NPLs, modifications in the synthesis method were endeavored. The injection timing and the TOP/Cu ratio (e.g., 5, 10, 20, and 50) of the dopant precursor was varied to achieve the successful doping in five ML CdSe NPLs. The detailed information about the synthesis of these dopant precursors is provided in the Experimental Section. The major challenge in

the synthesis was to achieve pure population of five ML doped NPLs as the reactivity and timing of the addition of the dopant precursor during the nucleation/growth stage of NPL synthesis affects the quality of doped NPLs and influences the inseparable sub-populations present along with required five ML doped NPLs.

Figure 1a,b presents the UV–visible absorption and steady-state PL spectroscopy results of undoped and Cu-doped CdSe NPLs synthesized by using a TOP/Cu ratio of 10, respectively. The absorption spectra indicate that both the electron-heavy hole (e-hh) and electron-light hole (e-lh) transitions of the CdSe NPLs remained similar after doping. In addition, the PL emission spectra exhibit the band-edge emission peak at 553 nm with a full width half maximum of 10 nm for undoped NPLs whereas in doped NPLs along with a weak emission at  $\approx 554$  nm, there is a strong and broad Stokes-shifted dopant-emission peak at  $\approx 740$ –760 nm in the NIR region.

In addition to the dopant precursor with the TOP/Cu ratio of 10, the TOP/Cu ratios of 5 and 20 also lead to the successful doping in five ML CdSe NPLs along with the occurrence of a dominant and efficient dopant induced emission. However, with an increase in the TOP/Cu ratios (e.g.,  $\geq 20$ ), it is very difficult to achieve the nearly pure population of five ML NPLs, which is free from sub-populations of six ML NPLs and QDs (Figure S1, Supporting Information), which can occur as secondary products during synthesis. Therefore, the use of TOP/Cu ratio of  $\leq 10$  results in an NPL crude synthesis with lesser extra populations. The small percentage of extra QDs synthesized along with five ML doped NPLs can be removed by size-selective precipitation. For the case of TOP/Cu ratio of 10, effects of the change of dopant concentrations were also studied (Figure S2, Supporting Information). The Cu doping values with respect to total cations (Cd+Cu) are estimated by conducting ICP-MS analysis on the doped NPLs. Briefly, before conducting measurements the as synthesized doped-NPLs were washed several times in order to remove extra unreacted cadmium and copper ions. The change in the doping percentage alters the dopant emission contribution (percentage contribution of Cu emission in total integrated emission) and hence changes absolute PL QYs of the samples (Figure S2, Supporting Information). Figure 1c,d depicts the STEM images of both undoped and Cu-doped NPLs, respectively. From the STEM images, it is observed that both undoped and doped NPLs are rectangular shaped. The average dimensions for the undoped and Cu-doped CdSe NPLs having five ML thicknesses are  $39 \times 15$  nm<sup>2</sup> and  $46 \times 17$  nm<sup>2</sup>, respectively. Additional STEM images at variable Cu-doping levels are presented in the Supporting Information (Figure S3, Supporting Information).

In order to confirm the presence of Cu-dopant ions in these synthesized NPLs we performed the XPS studies on differently doped samples. Figure 2a shows the survey spectrum of Cu (1.6%) doped five ML CdSe NPLs, which indicates the presence of Cd, Cu, and Se in different states. Figure 2b depicts the high-resolution XPS spectra of Se 3d orbitals where the Se 3d peak splits into 3d<sub>3/2</sub> and 3d<sub>5/2</sub> peaks at 54.75 and 53.95 eV, respectively. Similarly in Figure 2c, 3d<sub>3/2</sub> and 3d<sub>5/2</sub> peaks (at 411.96 and 405.19 eV) corresponding to Cd 3d orbital are observed to remain unchanged to the undoped CdSe NCs.<sup>[28,29]</sup> To confirm the presence of Cu-dopant ion in the host CdSe, the

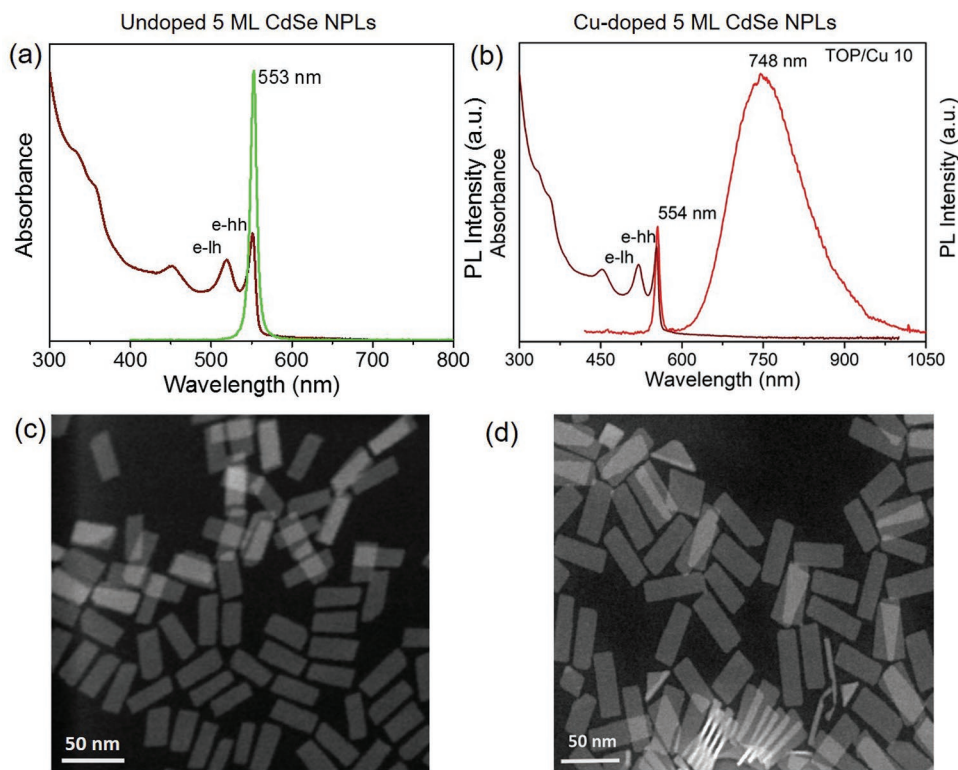


**Figure 1.** UV–visible absorption and PL emission spectra of a) undoped and b) 1.6% Cu-doped five ML CdSe NPLs. Scanning transmission electron microscopy (STEM) images of c) undoped and d) Cu-doped five ML CdSe NPLs.

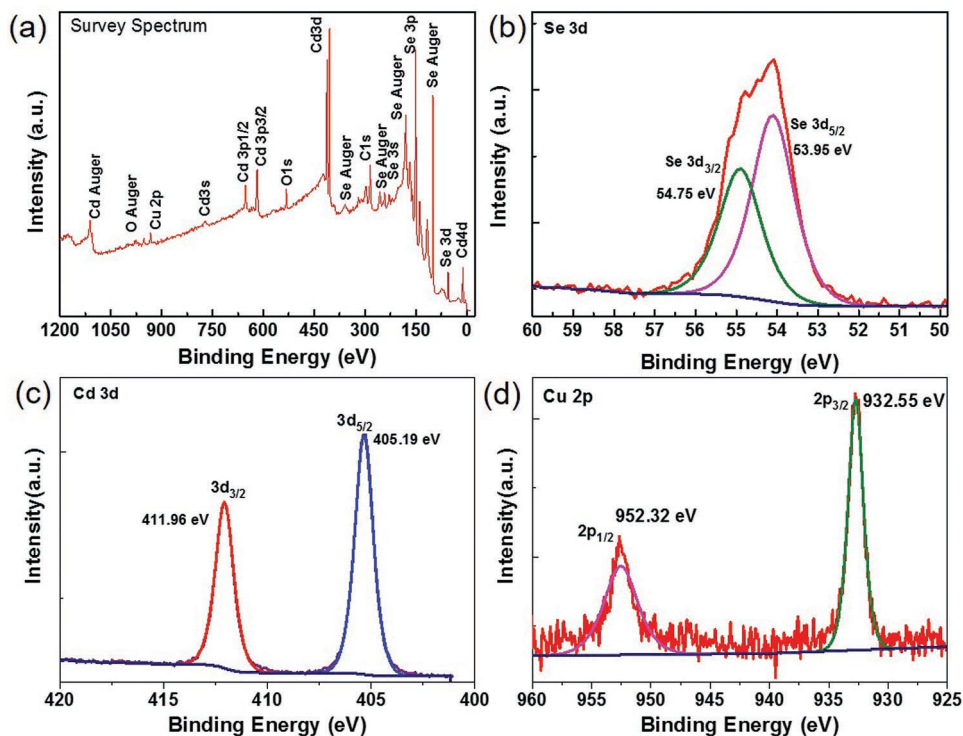


**Figure 2.** XPS spectra of Cu-doped five ML CdSe NPLs: a) survey spectrum and b–d) high-resolution XPS spectrum of Se 3d, Cd 3d, and Cu 2p orbitals.

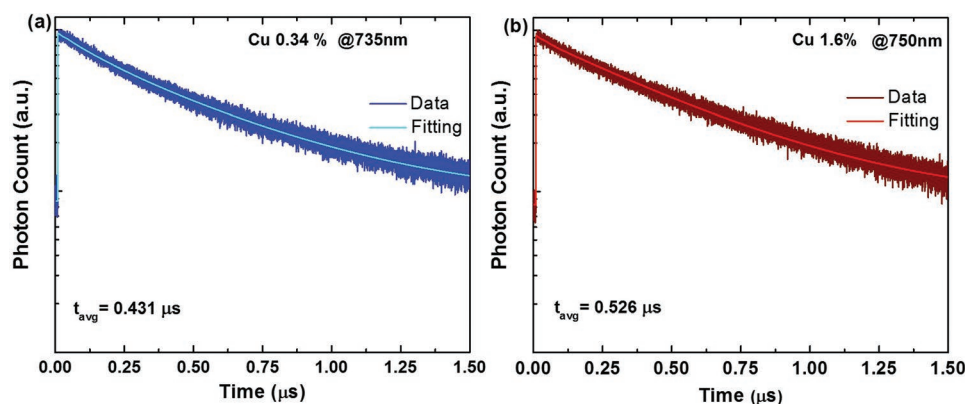


**Figure 3.** Time-resolved fluorescence decay curves for a) 0.34% and b) 1.60% Cu-doped five ML CdSe NPLs.

high-resolution XPS spectrum for Cu 2p orbitals has been carried out (Figure 2d). This shows that the Cu 2p orbital peaks split into  $2p_{1/2}$  and  $2p_{3/2}$  at 952.32 and 932.55 eV, respectively. While confirming the presence of Cu-dopant ions, XPS also allows us to identify the valence state of Cu-dopant ions, which is found to be very crucial in the understanding of the emission mechanism. Clearly, the absence of any satellite peak for Cu 2p orbitals confirms the valence state of Cu as +1 in our doped samples. Similar valence state has been previously reported by the majority of groups for Cu-doped CdSe NCs.<sup>[2,15,28,30,31]</sup>

Time-resolved fluorescence (TRF) spectroscopy was carried out to understand the emission kinetics of these doped NPLs. In Figure 3, the PL decay curves for doped NPLs at 0.34% and 1.60% Cu doping levels are shown. These decay curves for the dopant related emission are fitted with two exponentials and the calculated average lifetimes are 0.430 and 0.526  $\mu\text{s}$  for 0.34% and 1.60% of Cu-doping, respectively. The lifetimes for this Stokes-shifted emission clearly match with the Cu-based NCs lifetime reported in the literature.<sup>[13,15,32]</sup> Furthermore, the absence of any fast decay channel in the decay curves for these dopant emissions further supports the high PL QYs observed for these samples. The detailed TRF decay components are provided in Table S1 (Supporting Information).

Doping of Cu in CdSe NCs often results in a dual emission possessing contributions from both excitonic and dopant induced Stokes-shifted emissions.<sup>[13,15,33]</sup> In the literature, for the low doped CdSe NCs synthesized by a high-temperature heating method, the simultaneous emission from excitonic pathways along with the dominant Stokes-shifted dopant emission is observed. The appearance of excitonic emission in the doped samples is shown to be resulting from the small sub-population of undoped NCs in the ensemble of doped NCs.<sup>[33]</sup> For the case of the doped CdSe NPLs synthesized by using a high-temperature nucleation doping method, it is very difficult to achieve the full dopant emission. Furthermore, for the high-temperature nucleation doping method the use of higher concentration of the dopant precursor leads to creation of sub-populations (e.g., QDs and six ML NPLs), which are very difficult to separate from the intended five ML CdSe NPL populations. Therefore, to further increase the dopant emission in our already doped samples, postdoping at a high temperature has been investigated by following a previously reported recipe with slight modifications.<sup>[12]</sup> The detailed information

about the synthesis is provided in the Experimental Section. Figure 4a–d shows the absorption and PL emission spectra for two different Cu-doped CdSe NPLs before and after postdoping. Here, instead of the undoped cores, we used partially Cu-doped cores for the further increase of the dopant emission. As a control experiment, we also performed the postdoping with undoped five ML CdSe cores (Figure S4, Supporting Information). This control experiment with undoped core sample also results in nearly full percentage of the dopant emission. However, their PL QY was reduced from 30.0% to less than 1.0% after this postdoping (Figure S4, Supporting Information).

On the contrary, already doped samples (Cu-doped five ML CdSe NPLs synthesized by the nucleation doping method) showed marginal decrease in the PL QYs after undergoing similar postdoping experiments (which hereafter we term as doubly doped NPLs) (Figure 4). For the synthesis of these doubly doped samples the dopant precursor (TOP/Cu 10) used in the synthesis of the doped cores was again employed. Briefly, the addition of variable amount of the dopant precursor at 230 °C results in further increase in the dopant emission. As an example with small (e.g., 6  $\mu\text{L}$ ) addition of the dopant precursor, as seen in Figure 4a,b, very small increase in the dopant emission is observed. However, further increase in the amount of dopant precursor (e.g., 30  $\mu\text{L}$ ) leads to huge increase in the dopant-based emission. The initial concentration of the seed NPLs was same for both the cases as described in Figure 4. Figure 4d shows the shift of emission spectrum possessing a mixed contribution (i.e., excitonic and dopant emission) to purely dopant induced Stokes-shifted emission. Interestingly, in this case the dopant emission also possesses a huge redshift from 752 to 870 nm in the PL emission after the postdoping process. Similar redshift is also reported previously for the Cu-doped four ML CdSe NPLs with the increase in substitutional doping.<sup>[13]</sup> The absorption spectrum for this sample exhibits small broadening in the excitonic features (Figure 4c). However, both e-lh and e-hh peaks can be distinguishably seen in the absorption spectra. The STEM images for this sample are also recorded, which possess almost similar features before and after postdoping (Figure S5, Supporting Information). The PL QYs were also observed to remain similar before and after this postdoping procedure. The PL QYs for samples shown in Figure 4a,b were measured to be 41% and 38%, respectively,

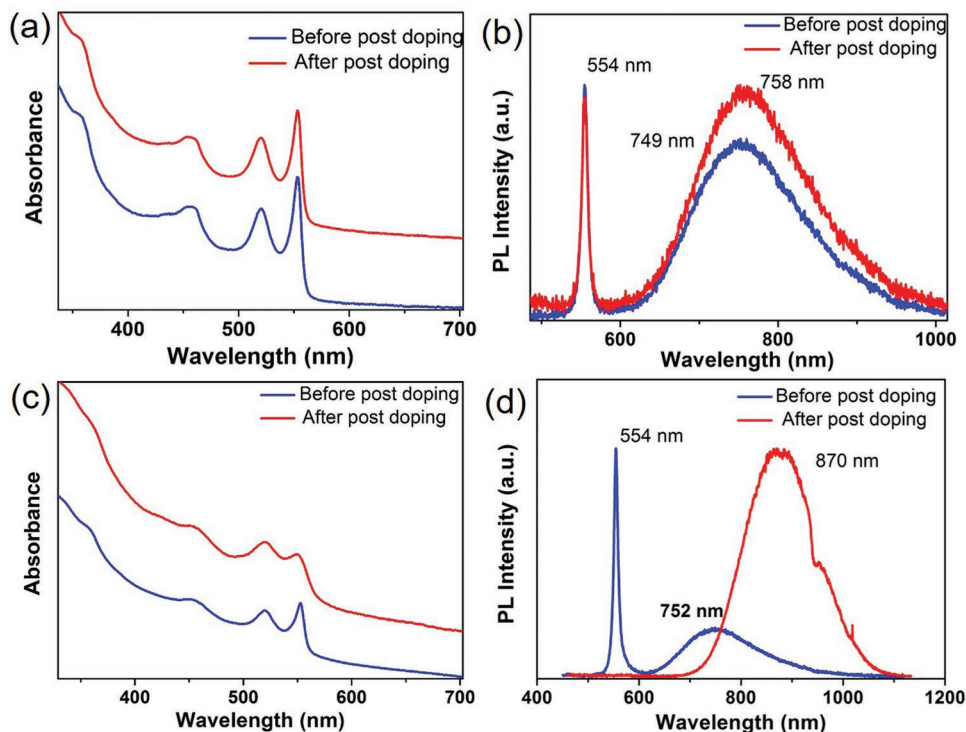


**Figure 4.** UV–visible absorption and PL emission spectra for Cu-doped five ML CdSe NPLs before and after postdoping on previously doped NPL samples after adding a,b) 6  $\mu\text{L}$  and c,d) 30  $\mu\text{L}$  of TOP/Cu (10) precursor.

whereas the PL QYs were found to be 29% and 27% for the samples shown in Figure 4c,d, respectively.

Recently Cu-doped materials have been shown to be promising candidates as luminophores for LSC applications.<sup>[1,15]</sup> In LSCs, the incorporated luminophore material absorbs the impinging solar light through a large surface and emits the light inside LSC panel, which is further wave guided via total internal reflection to the edges of the LSC slab where typically a photovoltaic cell is placed. In addition to the solar light concentration property, it is possible to fabricate semi-transparent LSC panels.<sup>[34]</sup> Semi-transparent nature of the LSCs offers effective solar energy generation solutions for heavily urbanized regions where they are implemented as window panels and facades in buildings as a part of zero-energy building concept.<sup>[35]</sup> However, since the first proposition in 1976,<sup>[35]</sup> LSCs are limited with the available material choices. Due to limited Stokes shift in the PL emission of the most luminophores, LSCs suffer significant reabsorption-related losses.<sup>[36,37]</sup> In this respect, a perfect LSC material should have a limited overlap between its absorption and emission while effectively absorbing a large portion of the solar spectrum.<sup>[38]</sup> 1D quantum confinement of NPLs creates a step-like absorption profile typical to 2D electron density of states, which creates perfect absorption profile with a sharp edge. However, practically zero Stokes shift in pristine NPLs makes it impossible to utilize this absorption profile as an LSC material. In our previous study, owing to their large Stokes-shifted emission, three and four ML NPLs have shown significantly good performance in LSCs as compared to similar Cu-doped QDs.<sup>[15]</sup> As compared to three and four ML NPLs, five ML NPLs are expected to offer higher LSC performance

by possessing more redshifted PL emission in the NIR region, along with larger solar spectrum coverage.

To evaluate the performance of five ML Cu-doped NPLs as LSC emitters, we calculated the external efficiency ( $\eta_{\text{ext}}$ ) for an LSC geometry having geometric gain factor of five in Figure 5. Here,  $\eta_{\text{ext}}$  characterizes the overall LSC efficiency of the solar flux absorption, delivering generated photons to the edges of the panel. In our calculations, lateral LSC dimensions are 10 cm  $\times$  10 cm and thickness is 5 mm for  $G = 5$  where  $G$  is the ratio between the large lateral face and the thin edges ( $G = L^2/4dL$ , where  $L$  is the side length and  $d$  is the thickness of the LSC panel) of the LSCs called the geometric gain factor. The flux gain or the concentration factor,  $C$ , is the product of these two quantities:  $C = \eta_{\text{ext}}G$ . Considering the solar light concentration, there is a tradeoff between  $\eta_{\text{ext}}$  and  $G$  since higher  $G$  requires thin LSCs, which results in lower  $\eta_{\text{ext}}$ . Here, we calculated  $\eta_{\text{ext}}$  since the window applications of LSCs targeting high power conversion efficiency require higher  $\eta_{\text{ext}}$ .  $\eta_{\text{ext}}$  is calculated as the product of the absorption efficiency,  $\eta_{\text{abs}}$ , and the internal efficiency,  $\eta_{\text{int}}$ . The details of the calculations can be found in the Supporting Information. In Figure 5a, the  $\eta_{\text{ext}}$  values for Cu-doped three, four, and five ML NPLs are calculated with the best reported in-solution PL QY values as 80%, 97%, and 67%, respectively. In Figure 5a,b, we aimed to achieve higher  $\eta_{\text{ext}}$  values for higher power conversion efficiency requiring applications. The maximum obtained 67% PL QY provides  $\eta_{\text{ext}} = 3.51\%$  with a projected 7.39%  $\eta_{\text{ext}}$  for unity PL QY. This projected value of 7.39% is higher than the predicted  $\eta_{\text{ext}}$  value for an LSC to be commercially viable.<sup>[39]</sup> To observe the effect of LSC geometry on the performance, we calculated

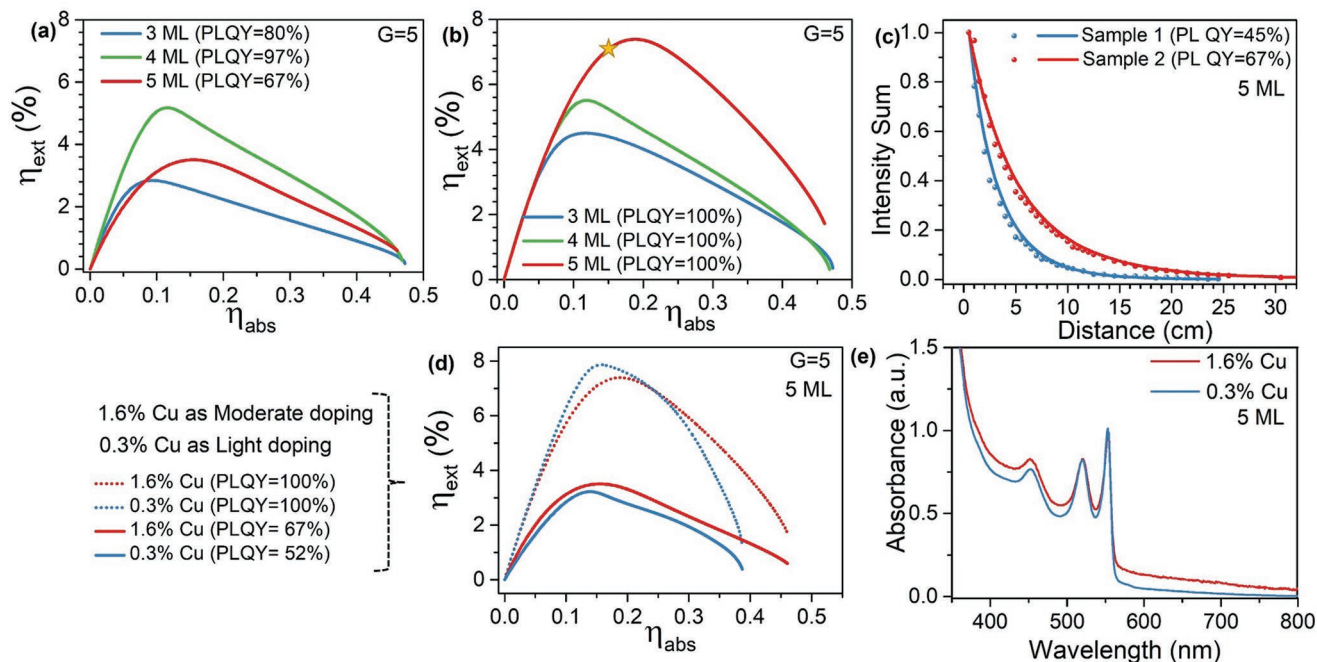


**Figure 5.** LSC performance assessment of Cu-doped five ML CdSe NPLs. External efficiency ( $\eta_{\text{ext}}$ ) comparison of Cu-doped NPLs with different thicknesses.  $\eta_{\text{ext}}$  calculated under different  $\eta_{\text{abs}}$  values for a) an LSC geometry having  $G = 5$  incorporated with Cu-doped NPLs having maximum observed in-solution PL QY values and b) unity PL QY case showing the maximum achievable  $\eta_{\text{ext}}$  with optimized synthesis methods. c) Reabsorption measurements for two different Cu-doped five ML NPLs having PL QY values of 67% and 45% in a 1D liquid waveguide. The concentration of the solutions is chosen to be close to the maximum efficiency point indicated with a star in (b). Due to this high concentration half-length values are limited ( $\approx 4.5$  cm). d) Comparison of  $\eta_{\text{ext}}$  for different doping concentrations in five ML NPLs shows that absorption tail observed e) with moderate doping has a limited effect on the LSC performance. Although, lightly doped NPLs slightly outperform moderately doped samples for the ideal PL QY case, experimentally observed higher PL QY value of moderately doped sample is expected to lead to better performance in LSCs.

LSC performance for  $G = 25$  in Figure S6 (Supporting Information). Despite the high geometric gain of the calculated LSC ( $G = 25$ ),  $\eta_{\text{ext}}$  values are more than 1% for all the emitters. Relatively low PL QY of five ML limits  $\eta_{\text{ext}}$  to 1.27%. Optimized synthesis routes can improve the PLQY of five ML and in Figure 5b we showed the possible  $\eta_{\text{ext}}$  values for unity PLQY cases. As expected, redshifted absorption and emission properties of five ML surpass three and four ML NPLs with maximum  $\eta_{\text{ext}}$  value of 7.39%.

Additional reabsorption studies have been conducted by following an earlier reported 1D liquid waveguide setup<sup>[1,15]</sup> for two different highly concentrated Cu-doped samples in Figure 5c. Here, we characterized the reabsorption losses to assess the LSC performance of our synthesized Cu-doped five ML samples using a previously reported 1D liquid waveguide setup with few modifications.<sup>[1,15]</sup> Since the PL emission of our doped NPLs overlaps with strong vibrational overtones of toluene solvent. Therefore, for all our reabsorption measurements we have used tetrachloroethylene as a solvent instead of toluene after following previous reports.<sup>[1,15]</sup> We calculated the reabsorption losses by measuring the PL spectra as a function of the optical path distance,  $L$ , up to 0.30 m. To compare these materials with the previously studied Cu-doped three and four ML NPL solutions, we prepared five ML NPL solution having an optical density of 1.0 ( $OD = 1.0$ ) over  $t = 1$  mm (thickness of the quartz cuvette) at their e-hh absorption peak. We marked the position of this particular concentration for 67%

efficient sample in Figure 5b with a star mark that is close to the peak position in the  $\eta_{\text{ext}}$  curve. We introduced the solution into fused silica waveguide making sure it is free from any air bubble. The excitation source was slid systematically at different values of  $L$ , where  $L$  is the optical path distance between the excitation source and the collection end of the waveguide. In this way, we characterized the reabsorption of emitted light while light travels through unexcited portion of the emitter solution. As we increased  $L$ , we observed a decrease in the PL emission intensity along with a redshift in PL emission spectra due to the reabsorption losses on the higher energy side of the spectrum (Figure S7, Supporting Information). The calculated half-length of five ML doped samples is found close to 4.5 cm (Figure 5c).

The agreement between our experimental reabsorption loss measurements of the Cu-doped five ML NPLs and the numerical modeling using Beer–Lambert law is a clear indication of the lack of waveguide-related losses, indicating that the main loss mechanism is the reabsorption losses. The details for the numerical modeling have been presented in our previous work.<sup>[15]</sup> The observed reabsorption losses are higher in our five ML doped samples as compared to our previously reported values for three and four ML doped NPL samples. We attribute this increase in the losses to the absorption tail emerging after Cu doping in five ML NPLs deviating from their inherent step-like absorption profile as shown in Figure S8 (Supporting Information). Regardless of the PL QY values for five ML samples, half-lengths for PL

intensity decrease are shorter than previously reported three and four ML Cu-doped NPL samples.<sup>[15]</sup>

In Figure 5d, we calculated the effect of the different doping concentrations of Cu-doped five ML NPLs on the LSC performance. Absorption spectra of the corresponding samples are provided in Figure 5e. Although lightly doped (0.3% Cu) sample slightly outperforms moderately doped (1.6% Cu) sample in ideal PL QY = 100% case, higher achieved PL QY of moderately doped sample (PL QY = 67%) results in a higher expected  $\eta_{\text{ext}}$  than lightly doped sample (PL QY = 52%) with measured PL QY values. This result indicates that the increased absorption tail in Cu-doped five ML NPLs does a limited effect on the LSC performance. However, heavy doping in host CdSe NPLs leads to very dominant intragap absorption tails due to direct photoexcitation from dopant ions to conduction band (CB).<sup>[1,13,40,41]</sup> Previously, this enhanced absorption tail is also shown to be contributing to reabsorption-related losses for LSCs.<sup>[1,25]</sup> Therefore, optimized dopant concentration (moderate to low) in five ML Cu-doped CdSe NPLs is required to achieve high PL QYs and near-step-like absorption profiles. Apart from this, any further improvement in the cleaning procedures of as synthesized Cu-doped five ML CdSe NPLs, which can successfully remove extra sub-populations, may also contribute to achieving near-step-like absorption profiles. Moreover, with the recent developments in the synthesis of CdSe-based NPLs, thicknesses are shown to be extended up to eight MLs.<sup>[42]</sup> Thus, the successful Cu-doping into these thicker NPLs would enable these doped NPLs as practical LSC emitters for future solar light harvesting applications.

### 3. Conclusions

In summary, we have demonstrated the Cu-doping in five ML thick CdSe NPLs using a high-temperature nucleation doping method. These Cu-doped five ML NPLs possess highly efficient and Stokes-shifted NIR emission. Using detailed XPS, ICP, steady-state, and time-resolved fluorescence spectroscopy studies we confirm the successful Cu<sup>+</sup> doping in five ML CdSe NPLs. Tuning the reactivity of the dopant precursor and hence controlling the reaction kinetics during nucleation step helps to achieve stable and reproducible synthesis. To achieve 100% dopant induced emission contribution from these doped NPLs, we proposed and demonstrated a two-step doping procedure. Reabsorption studies using highly concentrated solutions of five ML doped NPL samples show relatively reduced performance due to emerging absorption tail at the low energy side of the absorption spectrum. We also predicted the LSC performance of Cu-doped five ML NPLs and compared them with existing three and four ML NPLs for their possible use as LSC materials. Calculated  $\eta_{\text{ext}}$  value of 7.39% for unity PL QY is promising performance for five ML NPLs as a prospective LSC material. We believe that the further optimization in synthesis and removal of the extra populations can help to achieve ideal five ML Cu-doped CdSe NPLs for practical LSC applications.

### 4. Experimental Section

**Chemicals Used:** Cadmium nitrate tetrahydrate, sodium myristate, technical grade 1-octadecene (ODE), selenium, cadmium acetate

dihydrate, copper (II) acetate, trioctylphosphine (TOP), and technical grade oleic acid (OA) were purchased from Sigma-Aldrich. Methanol, ethanol, acetone, and hexane were purchased from Merck Millipore.

**Preparation of Cadmium Myristate:** The cadmium myristate was prepared by following the existing recipe in the literature.<sup>[18]</sup> It was made by dissolving 1.23 g of cadmium nitrate tetrahydrate in 40 mL of methanol and 3.13 g of sodium myristate in 250 mL of methanol. When both the mixtures were completely dissolved, their mixing was started and the solution was kept on strong stirring for 1 h. After that solution was centrifuged and precipitates were dissolved in methanol. The resulting product was washed for three times in order to remove the excess precursors. Finally, the white precipitates were kept in the vacuum overnight for complete drying.

**Synthesis of Cu-Doped Five ML Thick CdSe Nanoplatelets:** For this synthesis of doped NPLs, 340 mg of cadmium myristate and 27 mL of ODE were added in a 100 mL three-neck flask. The solution was degassed and stirred at 95 °C under vacuum for 1 h so that volatile solvents could be evaporated and the cadmium myristate could completely dissolve. Then the temperature of reaction mixture was raised to 250 °C under argon flow and at 130 °C a known amount of Cu precursor was added. After reaching 250 °C, 3 mL of 0.3 mmol of Se-ODE precursor was quickly injected. After 1 min growth at this temperature 160 mg of cadmium acetate was added. Thereafter the solution was kept at 250 °C for 7 min, and the reaction was terminated by adding 1 mL of OA. Then solution was cooled using water bath until it reached to room temperature. The precipitation of resulting CdSe NPLs was carried out with the addition of acetone and finally the cleaned NPLs were dispersed in toluene.

**Dopant Precursor:** Copper dopant precursor was synthesized by following the previously reported method.<sup>[15]</sup> However, TOP/Cu molar ratio was tuned in this study. Typically TOP/Cu ratios 5, 10, 20, and 50 were used.

**Selenium Precursor:** For the synthesis of doped and undoped five ML NPLs, selenium precursor was prepared by following the literature with slight modifications.<sup>[43]</sup> In the case of doped NPLs, Se powder (3 mmol) and ODE (30 mL) were mixed in a 50 mL three-neck flask. After stirring and argon bubbling for 10 min, the flask was set to 180 °C. The reaction was kept at 180 °C for overnight. Subsequently, it was stopped and cooled down to room temperature. The Se plus ODE solution was kept in darkness before using it. For the typical synthesis of undoped NPLs, selenium precursor with the same molar ratio was prepared at higher temperature of 205 °C.

**Postdoping in Five ML CdSe NPLs:** For postdoping studies, predoped and undoped five ML CdSe NPL cores were used. Briefly, samples having a known optical density were precipitated with ethanol and added in 1 mL of hexane. To this solution, 5 mL of ODE was added and the mixture was degassed at 95 °C for 30 min. Thereafter, the temperature of the sample was raised to 230 °C under argon and different amounts of Cu precursor were added (TOP/Cu = 10) and kept at the same temperature for 20 min. After 20 min, the reaction was completed with the addition of 100  $\mu$ L of oleic acid followed by the addition of 5 mL toluene. Finally, these postdoped samples were cleaned twice with acetone and stored in toluene for further characterizations.

**Material Characterization:** The absorbance spectra (UV-visible) were recorded by a Varian-Cary 100 UV-visible spectrophotometer. The quantum yield of different doped and undoped NPLs was measured using a previously reported procedure (de Mello method).<sup>[44]</sup> The PL emission and QY measurements were performed at an excitation wavelength of 400 nm using a Spectral Products monochromator integrated xenon lamp, a Hamamatsu integrating sphere, and an Ocean Optics Maya 2000 spectrometer. To find shape and size of NPLs, transmission electron microscope images were recorded with a Tecnai G2-F30 model. A time-correlated single photon-counting system was used for collecting TRF measurements (Picoquant Fluotime 200). XPS measurements were conducted with Thermo K-alpha monochromatic high-performance X-ray photoelectron spectrometer. A Thermo X series II ICP-MS spectrometer was used to perform the elemental analysis.

## Supporting Information

Supporting Information is available from the Wiley Online Library or from the author.

## Acknowledgements

A.S. and M.S. contributed equally to this work. The authors gratefully acknowledge financial support from the Singapore National Research Foundation under the programs of NRF-NRFI2016-08. H.V.D. acknowledges support from ESF-EURYI and TUBA-GEBIP.

## Conflict of Interest

The authors declare no conflict of interest.

## Keywords

CdSe nanoplatelets, colloidal quantum wells, copper, doping, luminescent solar concentrators, near-infrared emission, Stokes shift

Received: May 17, 2019

Revised: July 31, 2019

Published online: August 20, 2019

- [1] L. R. Bradshaw, K. E. Knowles, S. McDowall, D. R. Gamelin, *Nano Lett.* **2015**, *15*, 1315.
- [2] K. E. Knowles, K. H. Hartstein, T. B. Kilburn, A. Marchioro, H. D. Nelson, P. J. Whitham, D. R. Gamelin, *Chem. Rev.* **2016**, *116*, 10820.
- [3] X. Wang, X. Yan, W. Li, K. Sun, *Adv. Mater.* **2012**, *24*, 2742.
- [4] R. W. Meulenberg, T. van Buuren, K. M. Hanif, T. M. Willey, G. F. Strouse, L. J. Terminello, *Nano Lett.* **2004**, *4*, 2277.
- [5] J. F. J. Suyver, S. F. S. Wuister, J. J. Kelly, A. Meijerink, *Phys. Chem. Chem. Phys.* **2000**, *2*, 5445.
- [6] K. Nose, T. Omata, O. Y. M. Shinya, *J. Phys. Chem. C* **2009**, *113*, 3455.
- [7] G. K. Grandhi, R. Tomar, R. Viswanatha, *ACS Nano* **2012**, *6*, 9751.
- [8] A. M. Smirnov, A. D. Golinskaya, P. A. Kotin, S. G. Dorofeev, V. V. Palyulin, V. N. Mantsevich, V. S. Dneprovskii, *J. Lumin.* **2019**, *213*, 29.
- [9] A. Singh, R. Kaur, O. P. Pandey, X. Wei, M. Sharma, *J. Appl. Phys.* **2015**, *118*, 044305.
- [10] M. Kaur, A. Sharma, M. Olutas, O. Erdem, A. Kumar, M. Sharma, H. V. Demir, *Nanoscale Res. Lett.* **2018**, *13*, 1.
- [11] J. Liu, Q. Zhao, J.-L. Liu, Y.-S. Wu, Y. Cheng, M.-W. Ji, H.-M. Qian, W.-C. Hao, L.-J. Zhang, X.-J. Wei, S.-G. Wang, J.-T. Zhang, Y. Du, S.-X. Dou, H.-S. Zhu, *Adv. Mater.* **2015**, *27*, 2753.
- [12] L. Yang, K. E. Knowles, A. Gopalan, K. E. Hughes, M. C. James, D. R. Gamelin, *Chem. Mater.* **2016**, *28*, 7375.
- [13] M. Sharma, M. Olutas, A. Yeltik, Y. Kelestemur, A. Sharma, S. Delikanli, B. Guzelurk, K. Gungor, J. R. McBride, H. V. Demir, *Chem. Mater.* **2018**, *30*, 3265.
- [14] R. Mazzaro, A. Vomiero, *Adv. Energy Mater.* **2018**, *8*, 1801903.
- [15] M. Sharma, K. Gungor, A. Yeltik, M. Olutas, B. Guzelurk, Y. Kelestemur, T. Erdem, S. Delikanli, J. R. McBride, *Adv. Mater.* **2017**, *29*, 1700821.
- [16] A. Yeltik, M. Olutas, M. Sharma, K. Gungor, H. V. Demir, *J. Phys. Chem. C* **2019**, *123*, 1470.
- [17] S. Ithurria, B. Dubertret, *J. Am. Chem. Soc.* **2008**, *130*, 16504.
- [18] S. Ithurria, M. D. Tessier, B. Mahler, R. P. S. M. Lobo, B. Dubertret, A. L. Efros, *Nat. Mater.* **2011**, *10*, 936.
- [19] C. S. Erickson, L. R. Bradshaw, S. McDowall, J. D. Gilbertson, D. R. Gamelin, D. L. Patrick, *ACS Nano* **2014**, *8*, 3461.
- [20] P. N. Tananaev, S. G. Dorofeev, R. B. Vasil'ev, T. A. Kuznetsova, *Inorg. Mater.* **2009**, *45*, 347.
- [21] C. She, I. Fedin, D. S. Dolzhenkov, P. D. Dahlberg, G. S. Engel, R. D. Schaller, D. V. Talapin, *ACS Nano* **2015**, *9*, 9475.
- [22] B. Martinez, M. G. Silly, M. Dufour, E. Izquierdo, T. Pons, E. Lhuillier, C. Delerue, S. Ithurria, *ACS Appl. Mater. Interfaces* **2019**, *11*, 10128.
- [23] A. H. Khan, V. Pinchetti, I. Tanghe, Z. Dang, B. Martín-García, Z. Hens, D. Van Thourhout, P. Geiregat, S. Brovelli, I. Moreels, *Chem. Mater.* **2019**, *31*, 1450.
- [24] M. B. Gopal, *Mater. Res. Express* **2015**, *2*, 085004.
- [25] K. E. Knowles, T. B. Kilburn, D. G. Alzate, S. McDowall, D. R. Gamelin, *Chem. Commun.* **2015**, *51*, 9129.
- [26] T. A. Cohen, T. J. Milstein, D. M. Kroupa, J. D. MacKenzie, C. K. Luscombe, D. R. Gamelin, *J. Mater. Chem. A* **2019**, *7*, 9279.
- [27] A. Yeltik, S. Delikanli, M. Olutas, Y. Kelestemur, B. Guzelurk, H. V. Demir, *J. Phys. Chem. C* **2015**, *119*, 26768.
- [28] Y. Wang, M. Zhukovskiy, P. Tongying, Y. Tian, M. Kuno, *J. Phys. Chem. Lett.* **2014**, *5*, 3608.
- [29] J. E. B. Katari, V. L. Colvin, A. P. Alivisatos, *J. Phys. Chem.* **1994**, *98*, 4109.
- [30] V. Lesnyak, C. George, A. Genovese, M. Prato, A. Casu, S. Ayyappan, A. Scarpellini, L. Manna, *ACS Nano* **2014**, *8*, 8407.
- [31] S. L. White, J. G. Smith, M. Behl, P. K. Jain, *Nat. Commun.* **2013**, *4*, 2933.
- [32] K. E. Knowles, H. D. Nelson, T. B. Kilburn, D. R. Gamelin, *J. Am. Chem. Soc.* **2015**, *137*, 13138.
- [33] P. J. Whitham, K. E. Knowles, P. J. Reid, D. R. Gamelin, *Nano Lett.* **2015**, *15*, 4045.
- [34] F. Meinardi, H. McDaniel, F. Carulli, A. Colombo, K. A. Velizhanin, N. S. Makarov, R. Simonutti, V. I. Klimov, S. Brovelli, *Nat. Nanotechnol.* **2015**, *10*, 878.
- [35] F. Meinardi, F. Bruni, S. Brovelli, *Nat. Rev. Mater.* **2017**, *2*, 1.
- [36] Y. Zhao, G. A. Meek, B. G. Levine, R. R. Lunt, *Adv. Opt. Mater.* **2014**, *2*, 606.
- [37] C. Yang, R. R. Lunt, *Adv. Opt. Mater.* **2017**, *5*, 1600851.
- [38] V. I. Klimov, T. A. Baker, J. Lim, K. A. Velizhanin, H. McDaniel, *ACS Photonics* **2016**, *3*, 1138.
- [39] K. Wu, H. Li, V. I. Klimov, *Nat. Photonics* **2018**, *12*, 105.
- [40] V. Pinchetti, Q. Di, M. Lorenzon, A. Camellini, M. Fasoli, M. Zavelani-Rossi, F. Meinardi, J. Zhang, S. A. Crooker, S. Brovelli, *Nat. Nanotechnol.* **2018**, *13*, 145.
- [41] H. D. Nelson, D. R. Gamelin, *J. Phys. Chem. C* **2018**, *122*, 18124.
- [42] A. Polovitsyn, Z. Dang, J. L. Movilla, B. Martín-García, A. H. Khan, G. H. V. Bertrand, R. Brescia, I. Moreels, *Chem. Mater.* **2017**, *29*, 5671.
- [43] D. Chen, Y. Gao, Y. Chen, Y. Ren, X. Peng, *Nano Lett.* **2015**, *15*, 4477.
- [44] J. C. de Mello, H. F. Wittmann, R. H. Friend, *Adv. Mater.* **1997**, *9*, 230.